MATHEMATICAL MODELING AND COMPUTING, Vol. 10, No. 2, pp. 400–409 (2023)

Ternary hybrid nanofluid flow caused by thermal radiation and mass transpiration in a porous stretching/shrinking sheet

Vishalakshi A. B.[1], Kopp M. I.[2], Mahabaleshwar U. S.[1], Sarris I. E.[3]

[1] *Department of Studies in Mathematics, Shivagangotri, Davangere University, Davangere 577007, India*
[2] *Institute for Single Crystals of the National Academy of Sciences of Ukraine, Nauky Ave. 60, Kharkov 61072, Ukraine*
[3] *Department of Mechanical Engineering, University of West Attica, 250 Thivon and P. Ralli Str., 12244 Athens, Greece*

(Received 27 October 2022; Revised 4 April 2023; Accepted 5 April 2023)

In the current analysis, ternary hybrid nanofluid flow with heat transfer under the influence of transpiration and radiation is explored. Partial differential equations (PDEs) of the current work are mapped by using a similarity variable to convert into ordinary differential equations (ODEs) form. The volume fractions of the ternary hybrid nanofluid are used in the entire calculation to achieve better results. The exact investigation of the momentum equation produces the domain value. The impact of thermal radiation is considered under energy equation and solved analytically with solution domain to yield the temperature profile. Graphical representations can be used to evaluate the effects of the factors thermal radiation, heat source or sink, and porous media. The present work is taken into consideration for numerous industrial applications.

Keywords: *ternary hybrid nanofluid; mass transpiration; porous medium; thermal radiation; stretching/shrinking sheet.*

2010 MSC: 76D05, 76D10, 76N20 **DOI:** 10.23939/mmc2023.02.400

1. Introduction

Stretching sheet issues with non-viscous fluids have several implications, including the manufacturing of glass, fibre, and plastic and rubber sheets. Researchers' interest in sheet stretching difficulties is demonstrated by their observation of these various applications. Sakiadis [1, 2] is considered the father of the problems with stretching sheet. Crane [3] furthered this work by simulating the flow of a fluid over a sheet that is stretching or contracting. Numerous studies on stretching sheet issues are undertaken with the aid of these two articles [4–8], because of the potential for their use in many industrial processes, examination of flows resulting from stretched surfaces through heat transfer is taken into consideration. The quality of the material has a significant impact on how quickly it stretches in hot or cold fluids. Maxwell [9] made the observation that improving fluid thermal conductivity can be done by suspending a variety of materials with superior conductivity, such as solid particles. In more recent times, Choi and Eastman [10] advanced the idea of nanofluid as a novel type of heat transfer fluid.

Recently, there has been a lot of interest in the problem of MHD nanofluid boundary layer flow over a stretching/shrinking sheet [11–18]. Alias and Hafidzuddin [14] considered the problem of a magnetohydrodynamic (MHD) induced Navier slip flow over a non-linear stretching/shrinking sheet with the existence of suction. Khashi'ie N. S. et al. [15] studied the influence of suction on the flow, heat, and mass transfer characteristics over a permeable, shrinking sheet immersed in a doubly stratified micropolar fluid. Jalali et al. [16] studied magnetohydrodynamics (MHD) stagnation point flow in a porous medium with velocity slip. Yahaya et al. [17] analyzed numerical solutions for the flow of an Ag-CuO/H_2O hybrid nanofluid over a stretching sheet with suction, a magnetic field, double stratification, and multiple slip effects. Nithya and Vennila [18] considered the steady, incompressible,

two-dimensional hydromagnetic boundary layer flow of nanofluid passing through a stretched sheet under the influence of viscous and ohmic dissipations.

The concept of a hybrid nanofluid that contains several nanoparticles scattered in the base fluid and is expected to provide additional significant thermophysical and rheological characteristics as well as increasing heat transfer capabilities, has been proposed as a means of amplifying nanofluid. Both Khan et al. [19] and Jamaludin et al. [20] investigated hybrid nanofluids in various flow scenarios. A hybrid nanofluid algebraically decaying approach was developed by Mahabaleshwar et al. [21]. As nanofluid technology developed, three different types of nanofluids were mixed with a base fluid to create ternary hybrid nanofluid. According to Shakya et al. [22], the detected nanoparticles submerged in water accelerate the heat transmission rate. Understanding the size and shape of the nanoparticles is useful. The pioneer model, introduced by Hamilton and Crosser [23]. The properties of alumina, copper oxide, and titanium oxide nanoparticles that carry water were studied by Kumar [24]. Abbasi et al. [25] and Sahoo [26] have also published research on ternary hybrid nanofluid in a comparable field. The Casson fluid, which has specific properties and is used to describe fluid behavior that deviates from Newtonian behavior. In 1995, Casson presented this model for the flow of viscoelastic fluid. Fuel engineers abandoned this model when describing adhesive slurries. View a few of the most current studies by referencing [27–29].

Following analysis of the aforementioned studies, the current paper examines the flow of Casson fluid with heat transfer while ternary hybrid nanoparticles are present. The ODEs are obtained from PDEs with the help of similarity variables. There is proposed an example of analytical solution. The domain and temperature profile in terms of confluent hypergeometric equation with Biot number are obtained.

2. Mathematical model and solution

Casson fluid flow follows a steady state 2D flow created by a sheet that is stretching with velocity at u_w. The mass transfer speed at the plate's surface is also v_w. For instance, $v_w = 0$, $v_w > 0$, and $v_w < 0$ represent impermeable, suction, and injection examples, respectively. According to Fig. 1, three distinct shaped nanoparticles are injected into a fluid flow. The governing equations for the boundary layer include the equation of continuity and Navier's Stokes equation, which can be defined as follows [34, 35]:

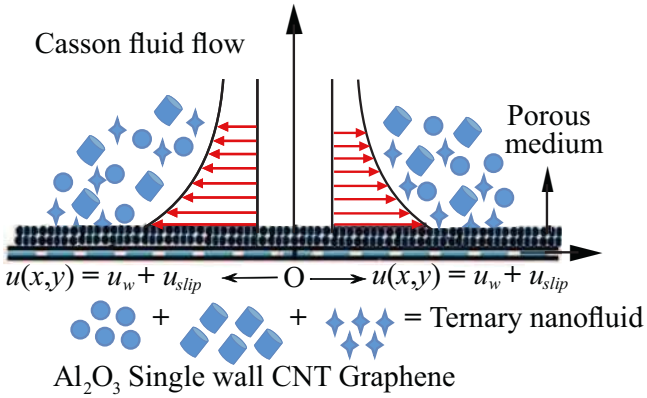

Fig. 1. Physical model of Casson fluid flow.

$$\frac{\partial u}{\partial x} + \frac{\partial v}{\partial y} = 0, \tag{1}$$

$$u\frac{\partial u}{\partial x} + v\frac{\partial u}{\partial y} = -\frac{1}{\rho_{tnf}}\frac{\partial p}{\partial x} + \frac{1}{\rho_{tnf}}\left(1 + \frac{1}{\Lambda}\right)\frac{\partial^2 u}{\partial y^2} - \frac{\mu_{tnf}}{K\rho_{tnf}}u, \tag{2}$$

$$u\frac{\partial T}{\partial x} + v\frac{\partial T}{\partial y} = \frac{\kappa_{tnf}}{(\rho C_p)_{tnf}}\frac{\partial^2 T}{\partial y^2} - \frac{1}{(\rho C_p)_{tnf}}\frac{\partial q_r}{\partial y} + \frac{Q_0\,(T - T_\infty)}{(\rho C_p)_{tnf}}, \tag{3}$$

suitable boundary conditions (B. Cs.) are [30]

$$\begin{aligned} u(x,y) &= u_w + u_{slip}, \quad v(x,y) = v_w \quad \text{at} \quad y = 0, \\ -\kappa\frac{\partial T}{\partial y} &= h\,(T_w - T) \quad \text{at} \quad y = 0, \\ u(x,y) &\to 0, \quad T \to T_\infty \quad \text{at} \quad y \to \infty, \end{aligned} \tag{4}$$

where u and v are the velocity components along x and y-direction, ρ_{thf} is the density of the ternary hybrid nanofluid, μ_{thf} is the dynamic viscosity of the ternary hybrid nanofluid, κ_{thf} is the ternary hybrid nanofluid's thermal conductivity, p is the pressure, K is the permeability of a porous medium and T is the temperature of the ternary hybrid nanofluid, $(\rho C_p)_{thf}$ is the ternary hybrid nanofluid's heat capacity.

In expression (4), $u_w = \pm ax$ indicates velocity of a sheet, $a = \text{const}$. Then the velocity gap slip at stretching sheet is given by

$$u_{slip} = b_s \delta u_y - c_s \delta^2 u_{yy} + \frac{4M}{\Gamma \rho_f \bar{\nu}} u_w, \tag{5}$$

where the 1st and 2nd order slip coefficients due to velocity shearing are as

$$b_s = 2(3 - \Gamma f^3)/(3\Gamma) - (1 - f^2)/K_n,$$

$$c_s = f^4/4 + (1 - f^2)/(2K_n^2),$$

where δ is the mean free path of gas molecules, $M = \rho_f v_w$ is mass flux at the wall, ρ_f is the density of the base fluid, Γ is the accommodation coefficient, ranging from 0 to 1, K_n is the Knudsen number, and $\bar{n}u$ is mean molecular speed.

Then the resulting slip velocity can be rewritten as

$$u_{slip} = b_s \delta \frac{\partial u}{\partial y} - c_s \delta^2 \frac{\partial^2 u}{\partial y^2} \pm m_1 ax, \tag{6}$$

where $m_1 = 4v_w/(\Gamma \bar{\nu})$.

Here is an introduction to the stream function ψ and similarity variable η

$$\psi(x, y) = x\sqrt{\nu a} f(\eta), \quad \theta(\eta) = \frac{T - T_\infty}{T_w - T_\infty}, \quad u = \frac{\partial \psi}{\partial y}, \quad v = -\frac{\partial \psi}{\partial x}. \tag{7}$$

$f(\eta)$, $\theta(\eta)$ are the dimensionless functions, T_w is the temperature at the wall, and T_∞ is the ambient temperature. Using Eq. (7),

$$u(x, y) = axf_\eta(\eta), \quad v = -\sqrt{\nu_f a} f(\eta). \tag{8}$$

The value of the heat flux, q_r, can be calculated using Rosseland's approximation as follows [31–33]:

$$q_r = -\frac{4\sigma^*}{3k^*} \frac{\partial T^4}{\partial y}. \tag{9}$$

The temperature T^4 expand as

$$T^4 = T_\infty^4 + 4T_\infty^3 (T - T_\infty) + 6T_\infty^2 (T - T_\infty)^2 + \ldots. \tag{10}$$

In Eq. (10), we neglected the higher order term to get the equation as

$$T^4 = -3T_\infty^4 - 4T_\infty^3 T. \tag{11}$$

Equation (11) is substituted into Eq. (9), and the resulting value is

$$\frac{\partial q_r}{\partial y} = -\frac{16\sigma^* T_\infty^3}{3k^*} \frac{\partial^2 T}{\partial y^2}. \tag{12}$$

On substituting Eqs. (7), (8) and (12) in Eq. (2) and (3) to get the following ODEs

$$\left(1 + \frac{1}{\Lambda}\right) \varepsilon_1 f_{\eta\eta\eta} - \varepsilon_2 f_\eta^2 + \varepsilon_2 f f_{\eta\eta} - \mathrm{Da}^{-1} \varepsilon_1 f_\eta = 0, \tag{13}$$

$$(\varepsilon_4 + R)\theta_{\eta\eta} + \mathrm{Pr}\, \varepsilon_3 f \theta_\eta + Q \,\mathrm{Pr}\, \theta = 0, \tag{14}$$

associated B. Cs. reduces to

$$f(0) = -\frac{v_w}{\sqrt{\nu_f a}} = V_c, \quad f_\eta(0) = d + \delta_1 f_{\eta\eta}(0) + \delta_2 f_{\eta\eta\eta}(0), \tag{15}$$

$$f_\eta(\infty) = 0, \quad \theta(\infty) = 0, \quad \theta_\eta(0) = -\mathrm{Bi}\,(1 - \theta(0)),$$

where V_c is velocity of mass transpiration, $\mathrm{Da}^{-1} = \frac{\mu_f}{K\rho_f a}$ is the inverse Darcy number, $R = \frac{16\sigma^* T_\infty^3}{3k^*\kappa_f}$ is the radiation parameter, σ^* and k^* are the Stefan–Boltzmann constant and the mean absorption coefficient, respectively; $\delta_1 = b_s\delta\sqrt{\frac{a}{\nu_f}}$ and $\delta_2 = -c_s\delta^2\frac{a}{\nu_f}$ are the 1st and 2nd order slips, $d = (1+m_1)$ is the stretching/ shrinking parameter, $\mathrm{Pr} = \frac{\mu C_P}{\kappa_f}$ is the Prandtl number, $Q = \frac{Q_0}{\rho C_P a}$ is heat source/sink parameter, $\mathrm{Bi} = \frac{h}{\kappa}\sqrt{\frac{\nu}{a}}$ is the Biot number.

Additionally, the ternary nanofluid quantities are as follows [36–38]. Let the ternary hybrid ferrofluid be composed of three sorts of nanoparticles, denoted by indices 1, 2, and 3.

$$\begin{aligned}
\varepsilon_1 &= \frac{\mu_{tnf}}{\mu_f} = \frac{B_1\phi_1 + B_2\phi_2 + B_3\phi_3}{\phi},\\
\varepsilon_2 &= \frac{\rho_{tnf}}{\rho_f} = 1 - \phi_1 - \phi_2 - \phi_3 + \phi_1\frac{\rho_{sp_1}}{\rho_{bf}} + \phi_2\frac{\rho_{sp_2}}{\rho_{bf}} + \phi_3\frac{\rho_{sp_3}}{\rho_{bf}},\\
\varepsilon_3 &= \frac{(\rho C_p)_{tnf}}{(\rho C_p)_f} = 1 - \phi_1 - \phi_2 - \phi_3 + \phi_1\frac{(\rho C_p)_{sp_1}}{(\rho C_p)_{bf}} + \phi_2\frac{(\rho C_p)_{sp_2}}{(\rho C_p)_{bf}} + \phi_3\frac{(\rho C_p)_{sp_3}}{(\rho C_p)_{bf}},\\
\varepsilon_4 &= \frac{\kappa_{tnf}}{\kappa_f} = \frac{B_4\phi_1 + B_5\phi_2 + B_6\phi_3}{\phi},
\end{aligned}$$

where $\phi = \phi_1 + \phi_2 + \phi_3$ is the overall volume fraction is the summation of the volume concentration of three dissimilar kinds of nanoparticles.

$$\begin{aligned}
B_1 &= \frac{\mu_{nf_1}}{\mu_f} = 1 + 2.5\phi + 6.2\phi^2,\\
B_4 &= \frac{\kappa_{nf_1}}{\kappa_f} = \frac{\kappa_{sp_1} + 2\kappa_f - 2\phi\left(\kappa_f - \kappa_{sp_1}\right)}{\kappa_{sp_1} + 2\kappa_f + \phi\left(\kappa_f - \kappa_{sp_1}\right)},\\
B_2 &= \frac{\mu_{nf_2}}{\mu_f} = 1 + 13.5\phi + 904.4\phi^2,\\
B_5 &= \frac{\kappa_{nf_2}}{\kappa_f} = \frac{\kappa_{sp_2} + 3.9\kappa_f - 3.9\phi\left(\kappa_f - \kappa_{sp_2}\right)}{\kappa_{sp_2} + 3.9\kappa_f + \phi\left(\kappa_f - \kappa_{sp_2}\right)},\\
B_3 &= \frac{\mu_{nf_3}}{\mu_f} = 1 + 37.1\phi + 612.6\phi^2,\\
B_6 &= \frac{\kappa_{nf_3}}{\kappa_f} = \frac{\kappa_{sp_3} + 4.7\kappa_f - 4.7\phi\left(\kappa_f - \kappa_{sp_3}\right)}{\kappa_{sp_3} + 4.7\kappa_f + \phi\left(\kappa_f - \kappa_{sp_3}\right)}.
\end{aligned}$$

3. Analytical solution for momentum and energy equation

Let us assume the solution of Eq. (13) as follows [39, 40]

$$f(\eta) = V_c + d\frac{[1 - \exp(-\alpha\eta)]}{\alpha\left(1 + \delta_1\alpha - \delta_2\alpha^2\right)}, \tag{16}$$

On using Eq. (16) in Eq. (13) to yield the following 4th order solution

$$m\alpha^4 + n\alpha^3 + o\alpha^2 + p\alpha + q = 0. \tag{17}$$

Here

$$m = \delta_2\left(1 + \frac{1}{\Lambda}\right)\varepsilon_1, \quad n = -\left(\left(1 + \frac{1}{\Lambda}\right)\varepsilon_1\delta_1 + \delta_2\varepsilon_2 V_c\right),$$

$$o = \delta_1\varepsilon_2 V_c - \left(1 + \frac{1}{\Lambda}\right)\varepsilon_1 - \varepsilon_1\mathrm{Da}^{-1}\delta_2, \quad p = \varepsilon_2 V_c + \varepsilon_1\mathrm{Da}^{-1}\delta_1,$$

$$q = \varepsilon_2\left(1 + m_1\right) + \varepsilon_1\mathrm{Da}^{-1}.$$

As a result, the skin friction C_f is as follows [41, 42]

$$C_f\sqrt{Re_x} = -\left(1 + \frac{1}{\Lambda}\right)\frac{d\alpha}{\left(1 + \delta_1\alpha - \delta_2\alpha^2\right)}. \tag{18}$$

Now, consider a new variable in order to solve the Eq. (14) as [43–45]

$$\xi = \frac{\Pr}{\alpha^2}\exp(-\alpha\eta). \tag{19}$$

Applying (19) to the equation (14) we get the following equation:

$$(\varepsilon_4+R)\xi\frac{\partial^2\theta}{\partial\xi^2}+\left\{(\varepsilon_4+R)-\varepsilon_3\Pr\left(\frac{V_C\alpha(1+\delta_1\alpha-\delta_2\alpha^2)+d}{\alpha^2(1+\delta_1\alpha-\delta_2\alpha^2)}\right)+\frac{d\varepsilon_3}{(1+\delta_1\alpha-\delta_2\alpha^2)}\xi\right\}\frac{\partial\theta}{\partial\xi}+\frac{Q\Pr}{\alpha^2\xi}\theta=0. \tag{20}$$

The reduced B. Cs. become

$$\frac{\Pr}{\alpha}\theta_\eta\left(\frac{\Pr}{\alpha^2}\right)=\mathrm{Bi}\left(1-\theta\left(\frac{\Pr}{\alpha^2}\right)\right),\quad \theta(0)=0. \tag{21}$$

Using new notation

$$A=(\varepsilon_4+R)-\varepsilon_3\Pr\left(\frac{V_C\alpha\left(1+\delta_1\alpha-\delta_2\alpha^2\right)+d}{\alpha^2\left(1+\delta_1\alpha-\delta_2\alpha^2\right)}\right),\quad \beta=\frac{d}{(1+\delta_1\alpha-\delta_2\alpha^2)},$$

Equation (20) can be rewritten as

$$(\varepsilon_4+R)\,\xi\frac{\partial^2\theta}{\partial\xi^2}+\{A+\beta\varepsilon_3\xi\}\frac{\partial\theta}{\partial\xi}+\frac{Q\Pr}{\alpha^2\xi}\theta=0. \tag{22}$$

Solving Eq. (22) by using B. Cs. of Eq. (21), we obtain the following result:

$$\theta(\eta)=\frac{e^{-b\alpha\eta}\mathrm{Bi}\,M\left(b,1+D,-\beta\varepsilon_3\frac{\Pr}{\alpha^2}e^{-\alpha\eta}\right)}{(\mathrm{Bi}+b\alpha)M\left(b,1+D,-\beta\varepsilon_3\frac{\Pr}{\alpha^2}\right)-\frac{b\beta\varepsilon_3\Pr}{\alpha(1+D)}M\left(b+1,2+D,-\beta\varepsilon_3\frac{\Pr}{\alpha^2}\right)}, \tag{23}$$

where

$$b=\frac{B+\sqrt{B^2-\frac{4Q\Pr}{(\varepsilon_4+R)\alpha^2}}}{2},\quad B=\Pr\varepsilon_3\left(\frac{V_C\alpha\left(1+\delta_1\alpha-\delta_2\alpha^2+d\right)}{\alpha^2\left(1+\delta_1\alpha-\delta_2\alpha^2+d\right)}\right),\quad D=\sqrt{B^2-\frac{4Q\Pr}{(\varepsilon_4+R)\,\alpha^2}}.$$

4. Results and discussion

The current research takes into account tnf flow with heat transfer under the influence of mass transpiration and thermal radiation stands for a colloidal mixture of three different particle types: graphene, single-walled CNTs, and Al_2O_3. Ternary hybrid nanofluid is increases the efficiency of heat transfer. The ODEs of the problem is obtained from the mapping the PDEs equation with similarity variables. The solution domain is obtained from solving the momentum equation and then heat equation verified analytically to get the confluent hypergeometric equation with Biot number. The findings of the present work can be discussed in the following ways using these graphical representations.

Figures 2 and 3 depict α verses V_C and δ_1 for raising the values of m_1 respectively. We observe the dual nature behavior that is blue solid lines indicate upper branch of solution and red solid lines indicate the lower branch of solution. While the values of α are raising then the values of m_1 also raising for upper branch of solution but the case is reversed for lower branch of solution that is raising the values of α will decreases the values of m_1. It is also conducted that on increasing the values of V_C and δ_1 the domain α value also increases.

Figures 4 and 7 indicate $f(\eta)$ verses η for raising m_1, Λ, δ_1, and δ_2 respectively. In Figure 4 $f(\eta)$ decreases with raising m_1 values, also we observe the same behaviour at Figures 5 and 7 that is on raising $f(\eta)$ values decreases the values Λ, and δ_2. But this effect is reversed at Figure 6, here $f(\eta)$ raises with δ_1. Impact of $f_\eta(\eta)$ on η for various values of Λ, V_C, δ_1, and δ_2 respectively indicated at Figures 8–11. Figure 8 explains that raising the values of $f_\eta(\eta)$ lowers the values of Λ, similarly the same impact observed at Figures 9 and 10 that is raising $f_\eta(\eta)$ lowers the values of V_C, and δ_1. But this effect is reversed at Figure 11, here raising values of $f_\eta(\eta)$ raises the values of δ_2.

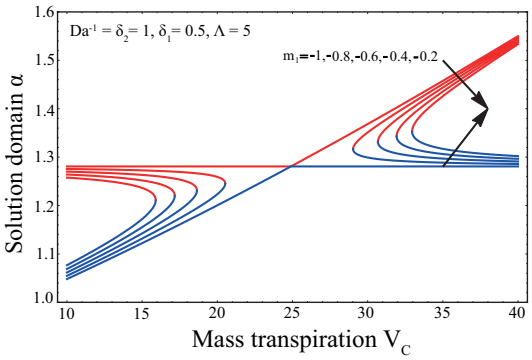

Fig. 2. Plots of domain α verses V_C for various m_1 values.

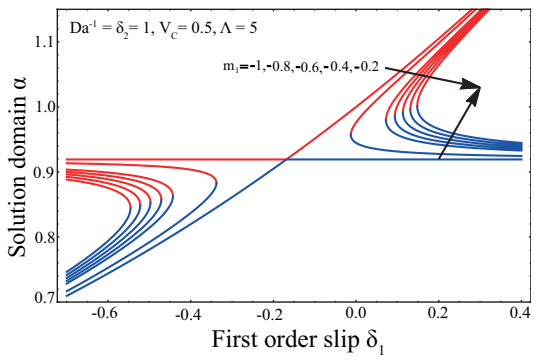

Fig. 3. Plots of domain α verses δ_1 for various m_1 values.

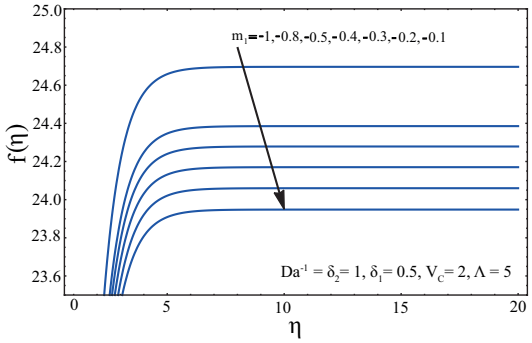

Fig. 4. $f(\eta)$ verses η for various m_1 values.

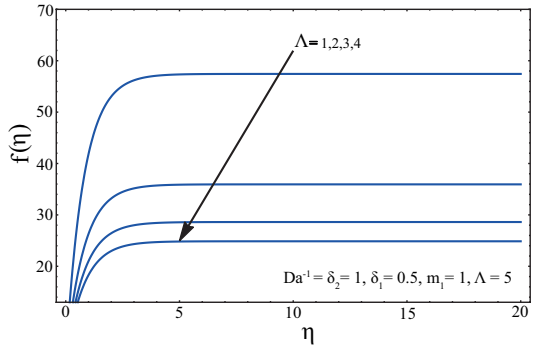

Fig. 5. $f(\eta)$ verses η for various Λ values.

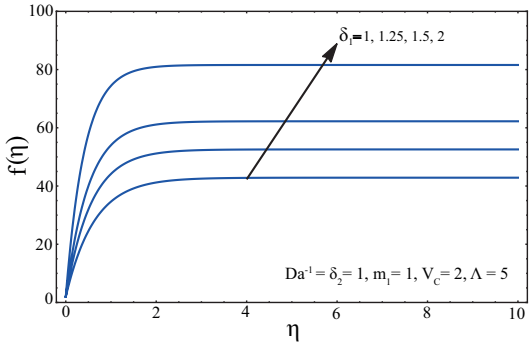

Fig. 6. $f(\eta)$ verses η for various δ_1 values.

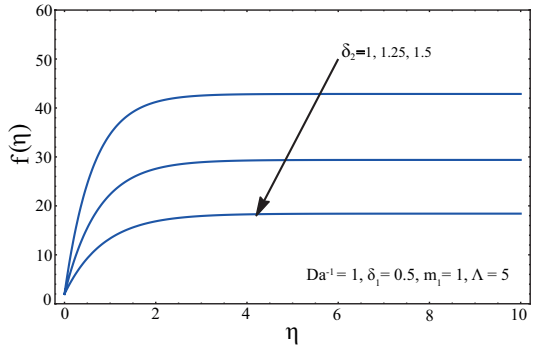

Fig. 7. $f(\eta)$ verses η for various δ_2 values.

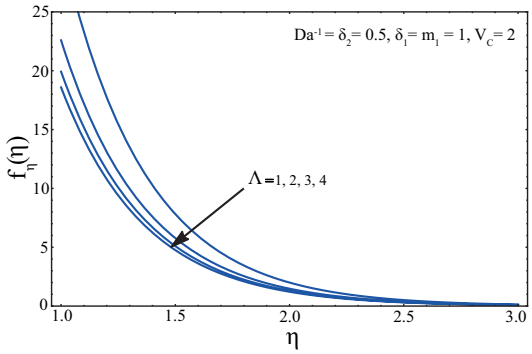

Fig. 8. $f_\eta(\eta)$ verses η for various Λ values.

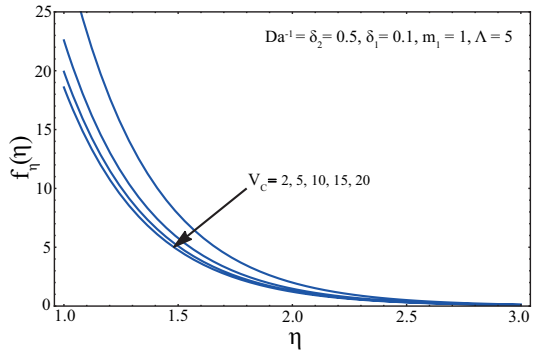

Fig. 9. $f_\eta(\eta)$ verses η for various V_C values.

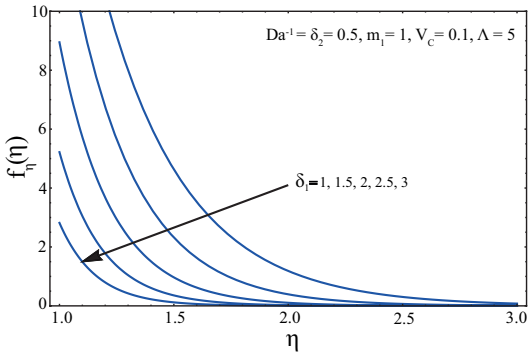

Fig. 10. $f_\eta(\eta)$ verses η for various δ_1 values.

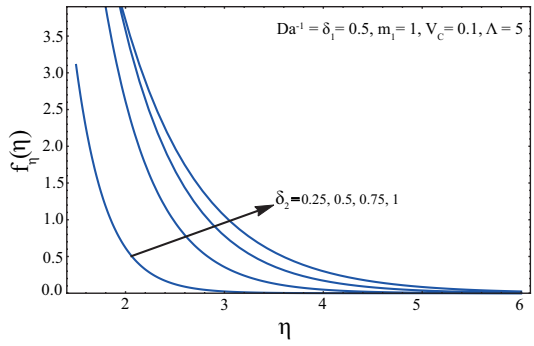

Fig. 11. $f_\eta(\eta)$ verses η for various δ_2 values.

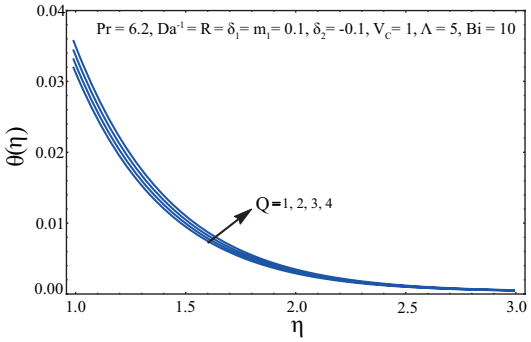

Fig. 12. $\theta(\eta)$ verses η for various Q values.

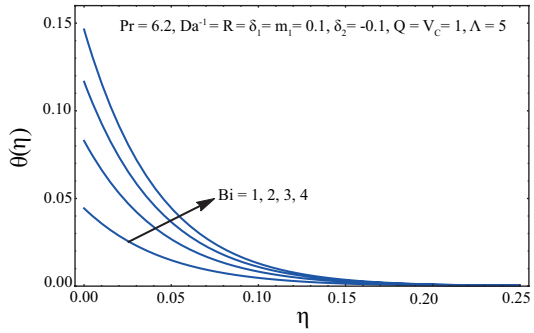

Fig. 13. $\theta(\eta)$ verses η for various Bi values.

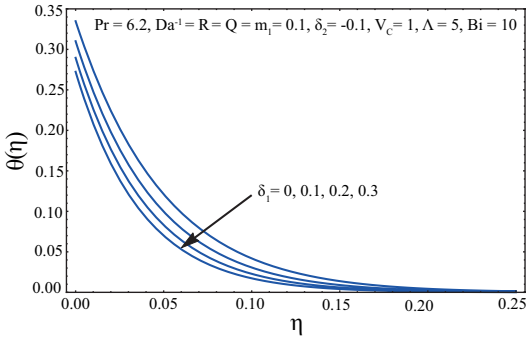

Fig. 14. $\theta(\eta)$ verses η for various δ_1 values.

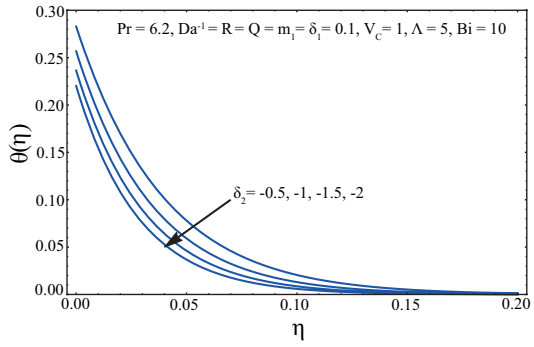

Fig. 15. $\theta(\eta)$ verses η for various δ_2 values.

The plots of $\theta(\eta)$ verses η for raising the values of Q, Bi, δ_1, and δ_2 respectively indicated at Figures 12–15. In Figure 12 raising $\theta(\eta)$ raises the values of Q, similarly the same impact observed at Figure 13 that is $\theta(\eta)$ increases with increasing the values of Bi. However, this impact is reversed in Figures 14 and 15, where $\theta(\eta)$ decreases as the values of δ_1, and δ_2 increase.

5. Conclusion

The study of Casson fluid flow with heat transfer in the presence of radiation and transpiration is what the current paper is all about. The ternary nanofluid materials are immersed in the flow of a fluid to get the better thermal efficiency of the fluid. The PDEs mapped with similarity variables to get ODEs and then these ODEs are solved analytically. The findings of the current research are then displayed using a graphical layout and with controlling parameters, at the end we concluded following points.

1. α increases with increasing the values of m_1 for upper branch of solution but this effect reversed for lower branch of solution.
2. Increasing V_C and δ_1 values raises the values of α.

3. Values of $f(\eta)$ decays with raising the m_1, Λ, and δ_2 values. But $f(\eta)$ raises with raising the $\delta_1$value.
4. $f_\eta(\eta)$ decays with raising the Λ, V_C, and δ_1 values. But $f_\eta(\eta)$ raises with raising the δ_2 values.
5. $\theta(\eta)$ raises with raising the Q, and Bi values. But $\theta(\eta)$ decays with raising δ_1, and δ_2 values.

Acknowledgments

The authors are grateful to an anonymous referee for their interest in this article and valuable comments.

[1] Sakiadis B. C. Boundary layer behaviour on continuous solid surfaces: I. Boundary layer equations for two-dimensional and axisymmetric flow. AIChE Journal. **7**, 26–28 (1961).

[2] Sakiadis B. C. Boundary layer behaviour on continuous solid surfaces: II. The boundary layer on a continuous flat surface. AIChE Journal. **7**, 221–225 (1961).

[3] Crane L. J. Flow past a stretching plate. Journal of Applied Mathematics and Physics (ZAMP). **21**, 645–647 (1990).

[4] Roşca N. C., Roşca A. V., Aly E. H., Pop I. Semi-analytical solution for the flow of a nanofluid over a permeable stretching/shrinking sheet with velocity slip using Buongiorno's mathematical model. European Journal of Mechanics – B/Fluids. **58**, 39–49 (2016).

[5] Siddheshwar P. G., Mahabaleshwar U. S. Effects of radiation and heat source on MHD flow of a viscoelastic liquid and heat transfer over a stretching sheet. International Journal of Non-Linear Mechanics. **40** (6), 807–820 (2005).

[6] Nandeppanavar M. M., Vajravelu K., Abel M. S., Siddalingappa M. N. Second order slip flow and heat transfer over a stretching sheet with non-linear Navier boundary condition. International Journal of Thermal Sciences. **58**, 143–150 (2012).

[7] Mahabaleshwar U. S., Anusha T., Sakanaka P. H., Bhattacharyya S. Impact of Lorentz force and Schmidt number on chemically reactive Newtonian fluid flow on a stretchable surface when Stefan Blowing and Thermal Radiation are Significant. Arabian Journal for Science and Engineering. **12**, 2427–12443 (2021).

[8] Mahabaleshwar U. S., Sneha K. N., Huang N.-H. An effect of MHD and radiation on CNT_S-water based nanofluid due to a stretching sheet in a Newtonian fluid. Case Studies in Thermal Engineering. **28**, 101462 (2021).

[9] Maxwell J. C. A Treatise on Electricity and Magnetism. Clarendon, Oxford (1873).

[10] Choi S. U. S., Eastman J. A. Enhancing thermal conductivity of fluids with nanoparticles. ASME Fluids Engineering Division. **231**, 99–105 (1995).

[11] Aly E. H. Existence of the multiple exact solutions for nanofluids flow over a stretching/shrinking sheet embedded in a porous medium at the presence of magnetic field with electrical conductivity and thermal radiation effects. Powder Technology. **301**, 760–781 (2016).

[12] Benos L. T., Polychronopoulos N. D., Mahabaleshwar U. S., Lorenzini G., Sarris I. E. Thermal and flow investigation of MHD natural convection in a nanofluid saturated porous enclosure: an asymptotic analysis. Journal of Thermal Analysis and Calorimetry. **143**, 751–765 (2021).

[13] Vishalakshi A. B., Mahabaleshwar U. S., Sarris I. E. An MHD fluid flow over a porous stretching/shrinking sheet with slips and Mass transpiration. Micromachines. **13** (1), 116 (2022).

[14] Alias N. S., Hafidzuddin M. E. H. Effect of suction and MHD induced Navier slip flow due to a non-linear stretching/shrinking sheet. Mathematical Modeling and Computing. **9** (1), 83–91 (2022).

[15] Khashi'ie N. S., Wahi N., Arifin N. M., Ghani A. A., Hamzah K. B. Effect of suction on the MHD flow in a doubly-stratified micropolar fluid over a shrinking sheet. Mathematical Modeling and Computing. **9** (1), 92–100 (2022).

[16] Japili N., Rosali H., Bachok N. MHD stagnation point flow over a stretching or shrinking sheet in a porous medium with velocity slip. Mathematical Modeling and Computing. **9** (4), 825–832 (2022).

[17] Yahaya R. I., Ali F. M., Arifin N. M., Khashi'ie N. S., Isa S. S. P. M. MHD flow of hybrid nanofluid past a stretching sheet: double stratification and multiple slips effects. Mathematical Modeling and Computing. **9** (4), 871–881 (2022).

[18] Nithya N., Vennila B. MHD Nanofluid boundary layer flow over a stretching sheet with viscous, ohmic dissipation. Mathematical Modeling and Computing. **10** (1), 195–203 (2023).

[19] Khan U., Shafiq A., Zaib A., Baleanu D. Hybrid nanofluid on mixed convective radiative flow from an irregular variably thick moving surface with convex and concave effects. Case Studies in Thermal Engineering. **21**, 100660 (2020).

[20] Jamaludin A., Naganthran K., Nazar R., Pop I. MHD mixed convection stagnation-point flow of Cu-Al_2O_3/water hybrid nanofluid over a permeable stretching/shrinking surface with heat source/sink. European Journal of Mechanics – B/Fluids. **84**, 71–80 (2020).

[21] Mahabaleshwar U. S., Vishalakshi A. B., Andersson H. I. Hybrid nanofluid flow past a stretching/shrinking sheet with thermal radiation and mass transpiration. Chinese Journal of Physics. **75**, 152–168 (2022).

[22] Shakya A., Yahya S. M., Ansari M. A., Khan S. A. Role of 1-Butanol on Critical Heat Flux Enhancement of TiO_2, Al_2O_3 and CuO Nanofluids. Journal of Nanofluids. **8** (7), 1560–1565 (2019).

[23] Hamilton R. L., Crosser O. K. Thermal Conductivity of Heterogeneous Two-Component Systems. Industrial and Engineering Chemistry Fundamentals. **1** (3), 187–191 (1962).

[24] Sahoo R. R., Kumar V. Development of a new correlation to determine the viscosity of ternary hybrid nanofluid. International Communications in Heat and Mass Transfer. **111**, 104451 (2020).

[25] Abbasi M., Heyhat M. M., Rajabpour A. Study of the effects of particle shape and base fluid type on density of nanofluids using ternary mixture formula: a molecular dynamics simulation. Journal of Molecular Liquids. **305**, 112831 (2020).

[26] Sahoo R. R. Thermo-hydraulic characteristics of radiator with various shape nanoparticle-based ternary hybrid nanofluid. Powder Technology. **370**, 19–28 (2020).

[27] Chakravarthala S. K. R., Sandeep N., Ali M. E., Nuhait A. O. Heat and mass transfer in 3-D MHD Williamson–Casson fluids flow over a stretching surface with non-uniform heat source/sink. Thermal Science. **23** (1), 281–293 (2019).

[28] Kumaran G., Sandeep N., Ali M. E. Computational analysis of magnetohydrodynamic Casson and Maxwell flows over a stretching sheet with cross diffusion. Results in Physics. **7**, 147–155 (2017).

[29] Ali M. E., Sandeep N. Cattaneo–Christov model for radiative heat transfer of magnetohydrodynamic Casson–ferrofluid: A numerical study. Results in Physics. **7**, 21–30 (2017).

[30] Hamid M., Usman M., Khan Z. H., Ahmad R., Wang W. Dual solutions and stability analysis of flow and heat transfer of Casson fluid over a stretching sheet. Physics Letters A. **383** (20), 2400–2408 (2019).

[31] Bataller C. R. Radiation effects for the Blasius and sakiadis flows with a convective surface boundary condition. Applied Mathematics and Computation. **206** (2), 832–840 (2008).

[32] Nandy S. K., Pop I. Effects of magnetic field and thermal radiation on stagnation flow and heat transfer of nanofluid over a shrinking surface. International Communications in Heat and Mass Transfer. **53**, 50–55 (2014).

[33] Anusha T., Huang H.-N., Mahabaleshwar U. S. Two dimensional unsteady stagnation point flow of Casson hybrid nanofluid over a permeable flat surface and heat transfer analysis with radiation. Journal of the Taiwan Institute of Chemical Engineers. **127**, 79–91 (2021).

[34] Pantokratoras A. Flow adjacent to a stretching permeable sheet in a Darcy–Brinkman porous medium. Transport in Porous Media. **80** (2), 223–227 (2009).

[35] Tamayol A., Hooman K., Bahrami M. Thermal analysis of flow in a porous medium over a permeable stretching wall. Transport in Porous Media. **85** (3), 661–676 (2010).

[36] Animasaun I. L., Yook S.-J., Muhammad T., Mathew A. Dynamics of ternary-hybrid nanofluid subject to magnetic flux density and heat source or sink on a convectively heated surface. Surfaces and Interfaces. **28**, 101654 (2022).

[37] Saleem S., Animasaun I. L., Yook S.-J., Qasem M. A.-M., Shah N. A., Faisal M. Insight into the motion of water conveying three kinds of nanoparticles on a horizontal surface: Significance of thermo-migration and Brownian motion of different nanoparticles. Surfaces and Interfaces. **30**, 101854 (2022).

[38] Elnaqeeb T., Animasaun I. L., Shah N. A. Ternary-hybrid nanofluids: significance of suction and dual-stretching on three-dimensional flow of water conveying nanoparticles with various shapes and densities. Zeitschrift für Naturforschung A. **76** (3), 231–243 (2021).

[39] Aly E. H. Dual exact solutions of graphene-water nanofluid flow over stretching/shrinking sheet with suction/injection and heat source/sink: Critical values and regions with stability. Powder Technology. **342**, 528–544 (2019).

[40] Aly E. H., Hassan M. A. Suction and injection analysis of MHD nano boundary-layer over a stretching surface through a porous medium with partial slip boundary condition. Journal of Computational and Theoretical Nanoscience. **11** (3), 827–839 (2014).

[41] Khan Z. H., Qasim M., Ishfaq N., Khan W. A. Dual Solutions of MHD Boundary Layer Flow of a Micropolar Fluid with Weak Concentration over a Stretching/Shrinking Sheet. Communications in Theoretical Physics. **67** (4), 449–457 (2017).

[42] Khan S. K., Abel M. S., Sonth R. M. Visco-elastic MHD flow, heat and mass transfer over a porous stretching sheet with dissipation of energy and stress work. Heat and Mass Transfer. **40**, 47–57 (2003).

[43] Chaim T. C. Magnetohydrodynamic heat transfer over a non-isothermal stretching sheet. Acta Mechanica. **122**, 169–179 (1997).

[44] Fang T., Yao S., Pop I. Flow and heat transfer over a generalized stretching/shrinking wall problem. Exact solutions of the Navier-Stokes equations. International Journal of Non-Linear Mechanics. **46** (9), 1116–1127 (2011).

[45] Hamid M., Usman M., Khan Z. H., Ahmad R., Wang W. Dual solutions and stability analysis of flow and heat transfer of Casson fluid over a stretching sheet. Physics Letters A. **383** (20), 2400–2408 (2019).

Течія потрійної гібридної нанорідини, викликана тепловим випромінюванням і масовою транспірацією в пористому листі, що розтягується/стискається

Вішалакші А. Б.[1], Копп М. Й.[2], Махабалешвар У. С.[1], Сарріс І. Е.[3]

[1] *Факультет математики, Університет Давангере, Шіваганготрі, Давангере, Індія 577 007*
[2] *Інститут монокристалів НАН України, пр. Науки 60, 61072 Харків, Україна*
[3] *Факультет машинобудування, Університет Західної Аттики, вул. Тівон та П. Ралі 250, 12244 Афіни, Греція*

У цій роботі досліджується течія потрійної гібридної нанорідини по пористому листу, що розтягується/стискається, з теплообміном під впливом транспірації та випромінювання. Використовуючи змінні подоби, основні рівняння в частинних похідних для цієї задачі перетворено у звичайні диференційні рівняння. Для отримання більш коректних результатів у обчисленнях використовувалися об'ємні частки потрійної гібридної нанорідини. Знайдено точний аналітичний розв'язок рівняння руху та визначено область його існування. Вплив теплового випромінювання розглядається в межах рівняння енергії та розв'язується аналітично для отримання температурного профілю. Подані у вигляді графіків результати використовуються для аналізу факторів впливу теплового випромінювання, джерела чи стоку тепла та пористості середовищ. Отримані у роботі результати можуть знайти широке застосування в різних галузях промисловості.

Ключові слова: *потрійна гібридна нанорідина; масова транспірація; пористе середовище; теплове випромінювання; розтягування/стиснення листа.*